Time-lapse Vertical Seismic Profiling in Well 2A at the CBRA

Shelby L. Peterie, Marcus Tamburro, Julian Ivanov, Richard D. Miller,
Brett Wedel, Connor Umbrell, and Cole Bunker

Kansas Geological Survey
1930 Constant Avenue
Lawrence, KS 66047

Report to

Dale Davis and Spencer Cronin
Burns & McDonnell
9400 Ward Parkway
Kansas City, MO 64114
816-839-9526

Open-File Report 2025–48 April 2025

This study was conducted in complete compliance with ASTM Guide D7128-05. All data, interpretations, and opinions expressed or implied in this report and associated study are reasonably accurate and in accordance with generally accepted scientific standards.

Time-lapse Vertical Seismic Profiling in Well 2A at the CBRA

Executive Summary

Over the past decade, time-lapse comparison of shear-wave velocity profiles calculated from passive seismic energy has provided generalized insights into overburden stability and, indirectly, void dynamics at legacy salt dissolution wells in Hutchinson, Kansas. Velocity variability at well 2A suggested dynamic changes in stress that could be related to variations in roof rock properties. Well 2A was redrilled in late 2022 to directly investigate possible causes of the consistently observed time-lapse variability and invasively evaluate any void migration above the salt interval. Three large voids were encountered in the salt, the shallowest of which has a roof at the salt–shale contact. Interference between unique stress fields radiating from these stacked voids could result in complex interactions in bedrock stress and, therefore, exhibit variations in shear-wave velocity over time.

Three-component, multi-offset and azimuth vertical seismic profile (VSP) data were acquired in Well 2A in February 2023 to identify reflecting interfaces and assess potential signals related to voids as a baseline for future monitoring surveys. Reflection-like events observed at various times in the vertical component of the VSP are approximately consistent with expected arrivals times for P-wave diffractions originating from the tops of three voids encountered drilling out this legacy wellbore. A follow-up VSP survey was acquired in November 2023 to assess any time-lapse changes in reflection characteristics (and, thus, changes in roof configuration). Changes in surface conditions between the two surveys sufficiently altered the source wavelet so that direct differencing of the two data sets was impossible. Qualitative comparison suggested little to no change in reflection characteristics of the upper void was evident between the two surveys. It was concluded that future VSP data should be collected using the exact source location (not just same offset) occupied during the baseline survey to optimize repeatability for differencing.

A VSP survey was collected in September 2024 with the source at approximately the same location as the baseline survey to improve source repeatability. Results from this most recent VSP survey are similar to the baseline survey but appear to be impacted by reduced receiver coupling downhole. Weatherstripping and a thin rubber coating were added to the band and downhole tool housing, respectively, prior to the baseline survey to reduce mechanical vibration in the transverse direction evident on the shear-wave VSPs. Reduced receiver coupling observed on later surveys is likely a result of wear to those additions, which was not expected to affect the vertical component. New weatherstripping and rubber coating added prior to future VSP surveys should improve coupling and, thus, repeatability/consistency with previous surveys.

Reflections from the three larger voids are evident in the 2024 VSP. Little to no change is observed in the void signatures since the baseline survey. Results from numerical modeling are consistent with the VSPs collected in well 2A, strengthening the original interpretation. Seismic modeling indicates that, due to the relatively large wavelength/Fresnel zone, subtle changes in diffraction amplitude and phase would be evident even with minimal horizontal growth of the upper void. Vertical migration of the void would result in destructive interference with the top of salt reflection and notably reduce the diffraction amplitude, which makes this method sensitive to any vertical migration of the upper void. It is likely that little or no vertical growth has occurred since the 2023 baseline VSP given the relatively consistent amplitude of the upper void diffraction.

Introduction

Passive multichannel analysis of surface waves (MASW) has been used at the Vigindustries Site (Carey Boulevard Research Area, CBRA) to estimate shear-wave velocity (Vs) at numerous legacy salt dissolution wells since 2013 to monitor for changes in bedrock stresses in the vicinity of the solution mined voids. Time-lapse comparison of Vs profiles has provided insights into consistency of overburden stability and, indirectly, void dynamics. Well 2A consistently experienced changes in velocity, most notably in 2014, suggesting changes could be related to variations in bedrock properties/stress. Well 2A was drilled out in late 2022 to allow direct investigation for possible causes of the consistently observed, inconsistent time-lapse variability. The three largest voids in the salt were penetrated at depths of 125-137, 143-161, and 191-215 m. Interference of the stress fields from these distinctly stacked voids could result in complex variations measured in bedrock stress—and, therefore, shear-wave velocity over time.

Vertical seismic profiling (VSP) is a direct downhole technique used for determining elastic velocities, mapping reflecting interfaces (contact between materials with different physical properties), and relating those to geologic structures in close proximity to a borehole (Hardage, 1985a; Stewart and DiSiena, 1989). For a traditional VSP, the source is located near the borehole and provides a measure of seismic properties and images very near (an offset distance that is small relative to the deepest sampling point in the borehole) to the wellbore. For an offset VSP, the source is located at various distances from the borehole with the farthest source location generally equal to the depth to the deepest sensor location. Three-component, multi-offset and azimuth VSP data were acquired in well 2A in February 2023 to map reflecting interfaces and assess signal characteristics related to voids. Reflection-like events observed in the vertical component of the 61 m source offset VSP were generally consistent with expected arrival times for compressional-wave (P-wave) diffractions returning from the tops of the three main voids encountered during drilling.

A follow-up VSP survey was acquired in November 2023 to search for any time-lapse changes in reflection characteristics (and, thus, changes in roof configuration or overburden). Source repeatability is crucial for direct differencing of VSPs to assess subtle changes in roof configuration (or lack thereof). To accommodate truck traffic at the elevator, the source location for this second monitoring VSP survey was again at 61 m but located in the hardpack parking area north of the road rather than the lawn south of the road. The change in source location affected the seismic wavelet characteristics, resulting in lower signal-to-noise ratio (S/N). Little or no change was evident in qualitative comparison of the reflection from the upper void (Peterie et al., 2024). It was determined that future VSP data should be collected using the source location established during the baseline survey to minimize changes unrelated to the voids and optimize repeatability for differencing (quantitative comparison).

In this report, numerical modeling was used to simulate a VSP survey in well 2A, producing various subsurface models designed to assess signatures from the top of the salt and the three primary voids for comparison with the real VSPs. A third VSP survey was conducted in September 2024 using the source location established during the baseline survey to optimize source repeatability. Data from the baseline and 2024 surveys were reprocessed with identical parameters to minimize/eliminate any changes in wavelet characteristics related to acquisition parameters or processing flow.

Geologic and Geophysical Setting

The Permian-aged Hutchinson Salt Member occurs in central Kansas, northwestern Oklahoma, and the northeastern portion of the Texas panhandle and is prone to and has an extensive history of natural and anthropogenic dissolution and formation of sinkholes (Figure 1). In Kansas, the Hutchinson Salt Member possesses an average net thickness of 75 m and reaches a maximum of more than 150 m in the southern part of the basin. Deposition occurring during fluctuating sea levels caused numerous halite beds, 0.2 to 3 m thick, to be formed interbedded with shale, minor anhydrite, and dolomite/magnesite. Individual salt beds may be continuous for only a few miles despite the remarkable lateral continuity of the salt as a whole (Walters, 1978).

The distribution and stratigraphy of the salt is well documented (Dellwig, 1963; Holdoway, 1978; Kulstad, 1959; Merriam, 1963). The salt reaches a maximum thickness in central Oklahoma and thins to depositional edges on the north and west, erosional subcrop on the east, and facies changes on the south. The increasing thickness toward the center of the salt bed is due to a combination of increased salt and more and thicker interbedded anhydrites. The Stone Corral Formation (a well-documented seismic marker bed) overlies the salt throughout Kansas where not eroded off (McGuire and Miller, 1989). Directly above the salt at this site is a thick sequence of Permian shale capped with a saturated interval of Pliocene-Pleistocene sediments.

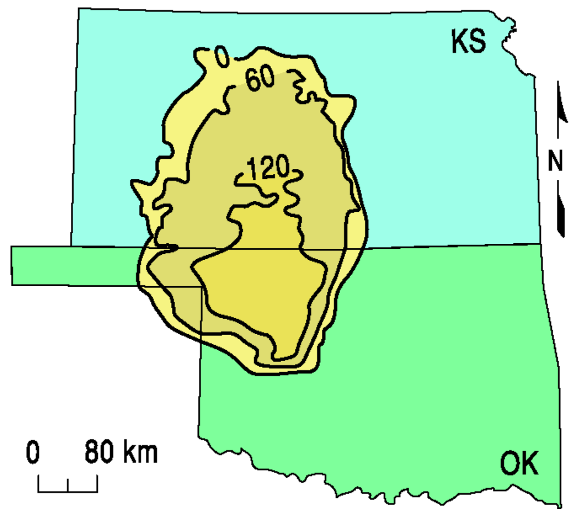

Figure 1. Approximate extent of salt formation, with contour intervals expressed in meters.

The upper 760 m of rock at this site is Permian shales (Merriam, 1963). The lower Wellington Shale (top at ~225 m deep), Hutchinson Salt (top at ~120 m deep), upper Wellington Shale (top at ~70 m deep), and Ninnescah Shale (top at ~15 m deep) make up the Permian portion of the section (Figure 2). Bedrock is defined as the top of the Ninnescah Shale with the unconsolidated Pliocene-Pleistocene Equus beds making up the majority of the approximate upper 15 m of sediment. Regionally, the thickness of Quaternary alluvium that fills stream valleys and paleosubsidence features extends from 0 to as much as 90 m, depending on the dimensions of the features.

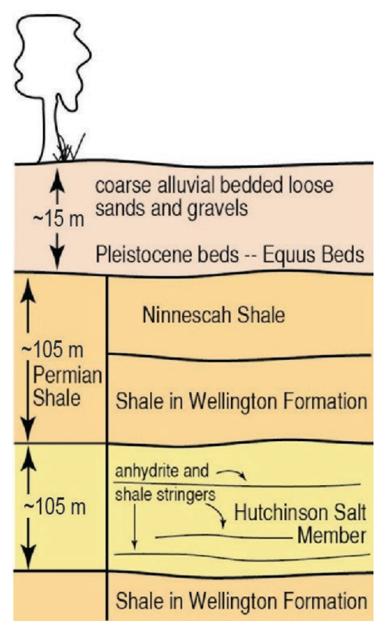

Figure 2. Generalized geology.

Recent dissolution of the salt and resulting subsidence of overlying sediments forming sinkholes has generally been associated with mining or saltwater disposal (Walters, 1978). Historically, these sinkholes can manifest themselves as a risk to surface infrastructure. The rate of surface subsidence can range from gradual to very rapid. Besides risks to surface structures, subsidence features potentially jeopardize the natural segregation of groundwater aquifers, greatly increasing their potential to negatively impact the environment (Whittemore, 1989, 1990). Natural sinkholes resulting from dissolution of the salt by localized leaching within natural flow systems that have been altered by structural features (such as faults and fractures) are not uncommon west of the main dissolution edge (Merriam and Mann, 1957).

Caprock and its characteristics are a very important component of any discussion concerning dissolution, subsidence, and formation of sinkholes. The Permian shales (Wellington and Ninnescah) that overlay the Hutchinson Salt Member are highly variable and can range from less than 60 m to more than 100 m thick in this area and are characterized as generally unstable when exposed to freshwater, being susceptible to sloughing and collapse (Swineford, 1955). These Permian shales tend to be red or reddish-brown and are commonly referred to as "red beds." Permian red beds are extremely impermeable to water and have provided an excellent seal between the freshwater of the Equus beds and the extremely water-soluble Hutchinson Salt Member. The modern-day expanse and mere presence of the Hutchinson Salt is due to the protection from freshwater provided by these red beds.

The basal contact of the Upper Wellington Formation shales provides key insights into the general strength of roof rock expected if dissolution-mined salt jugs (cavities or voids in the salt that form after salt has been dissolution mined in proximity to the wells) reach the top of the salt zone. Directly above the salt/shale contact is approximately 6 m thick dark-colored shale with joint and bedding cracks filled with red halite (Walters, 1978). Once an unsaturated brine encounters this shale layer, these red halite-filled joints and bedding planes are rapidly leached, leaving an extremely structurally weak layer.

Seismic Modeling

Finite-difference acoustic models (Virieux, 1986; Levander, 1988; and Zeng et al., 2011) were produced using ModelSeis software (developed at the KGS). These synthetic downhole data were instrumental in developing a defensible interpretation of the VSP data acquired for this study. To confidently establish and characterize the signals from top of salt and voids, synthetic models (Table 1) were produced to simulate (1) the reflection from the top of salt (salt–shale contact), (2) diffractions from the three main voids, and (3) superposition of signals from the top of salt and three voids. The third model (superposition of the top of salt signal and three voids) was re-run (Table 2) with (4) the same depth to top of the upper void but with the void top (roof) 50% wider, and (5) the upper void extending to just above the top of salt and into the shale caprock, with the intent to assess how these signatures would be affected if the upper void were to change.

Because of the presence of an unconsolidated layer greatly attenuated energy reaching bedrock, a two-layer model was used to represent the predominantly shale overburden and the Hutchinson Salt Member. Average Vp estimates for these layers were derived from a prior downhole survey in well 15B (Peterie et al., 2023). The source was located at the origin of the model, and the wavelet was the first derivative of the Gaussian function. Downhole receivers were located 61 m horizontally from the source and 3-109 m deep at 3 m intervals.

Table 1. Model parameters.

source frequency	150 Hz
layer 1 Vp	2400 m/s
layer 2 Vp	2800 m/s
layer 2 top	122 m

Table 2. Void parameters. Dimensions are listed width by height, and depth to top.

upper void	6 x 11, 126 m deep
middle void	18 x 18, 143 m deep
lower void	9 x 25, 191 m deep
void Vp	1500 m/s

Model 1—Two-layer model

Results from model 1 (Figure 3a) are straightforward and consist of the down-going direct wave (50-120 ms), the up-going top of salt reflection (120-140 ms), and the down-going reflection from the surface/top boundary of the model (140-210 ms). Reflections from the surface are typically not observable in real data due to attenuation in earth materials.

Model 2—Water-filled voids in a half-space

Results from model 2 (Figure 3b) are more complex and consist of: the down-going direct wave (50-120 ms); up-going diffractions from the top, middle, and lower voids (respectively, 120-140, 140-160, and 160-180 ms); and down-going reflections from the surface, as well as other reflection "multiples" not observed in real data.

Model 3—Two-layer model with water-filled voids

Three water-filled voids were added to the two-layer model to produce a record that should most closely simulate real data. As expected, results from model 3 (Figure 3c) are similar to model 2. The primary difference is the diffraction from the upper void is superimposed with the top of salt reflection. Constructive interference of these two events gives the appearance of a slightly greater diffraction amplitude, similar in amplitude to the diffraction from the middle void.

The results of model 3 are remarkably consistent with the baseline VSP acquired at well 2A and estimated/calculated diffraction arrival times for that well (Figure 4). Model arrival times of events are slightly earlier than arrival times of corresponding events in real data. This temporal difference is due to the designed absence of the slower unconsolidated layer in the model, effectively speeding up travel times. Otherwise, general arrival patterns and amplitudes of the reflection/diffractions in the model are nearly identical to those in real data, strengthening the validity of the original interpretation of the VSP (Peterie et al., 2023).

Model 4—Horizontal growth of upper void

Model 3 was modified to simulate horizontal/roof span growth of the upper void. The width of the void in the model increased 50% symmetrically around the borehole. Horizontal growth of the void (model 4, Figure 5b) results in a subtle change in the amplitude and phase of the diffraction from the upper void. The overall diffraction arrival pattern is similar to the original 6 m wide void (model 3, Figure 5a). These observations are expected given the size of the wavelength/Fresnel zone and associated relatively low horizontal resolution.

Model 5—Vertical migration of upper void

Model 3 was modified to simulate vertical growth/migration of the upper void. The top of the upper void was extended about 1 m above the salt–shale contact. Vertical growth of the upper void (model 5, Figure 5c) results in a notable change in the amplitude of the upper void diffraction. The amplitude variation is the result of destructive interference between the top of salt reflection and top of void diffraction from the upper void. This response represents a sensitive indicator of vertical migration of the upper void.

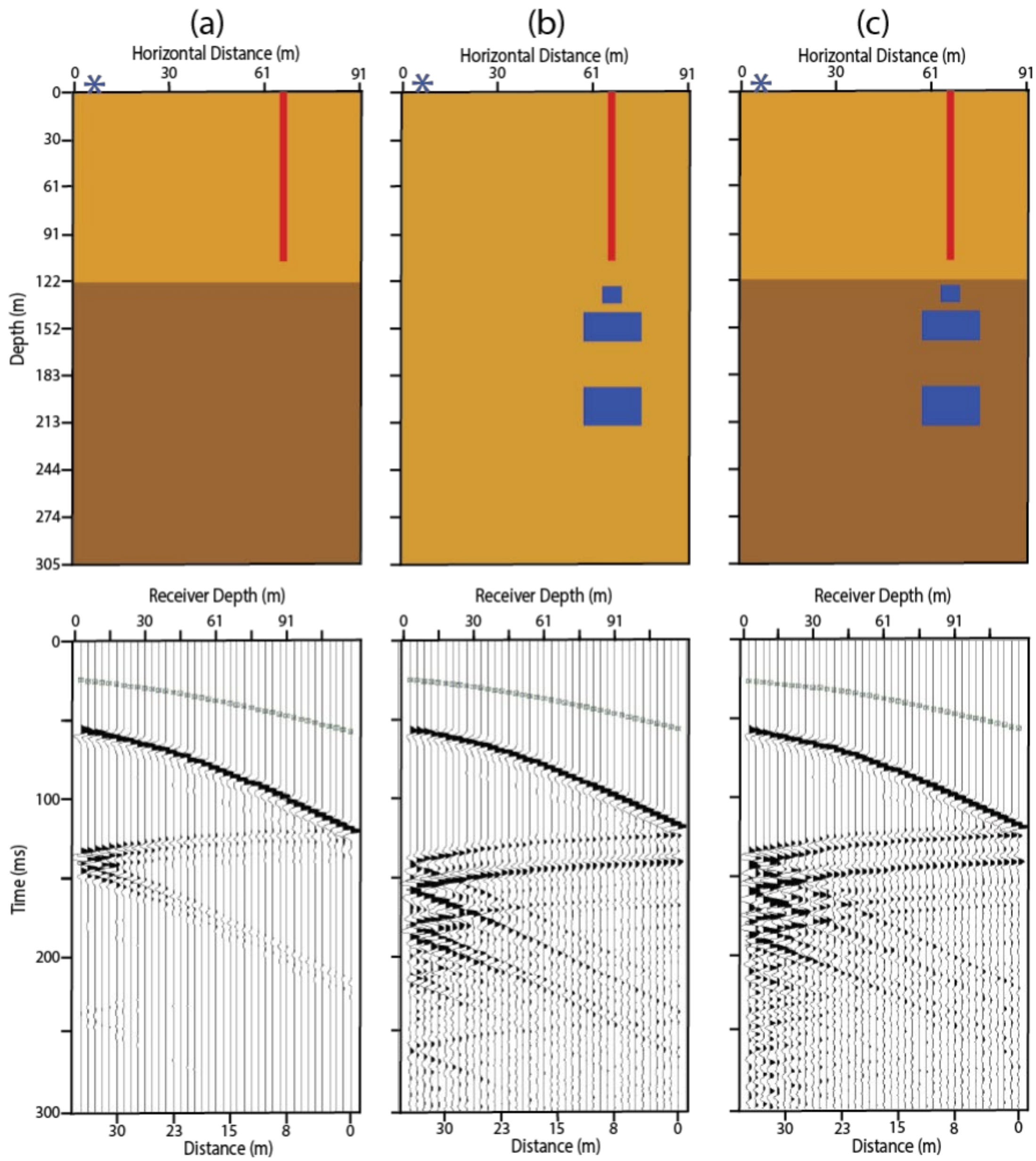

Figure 3. Graphical representation of the models (*top*, not to scale) and resulting synthetic seismograms (*bottom*) for (*a*) model 1, two-layer model; (*b*) model 2, water-filled voids in a half-space; and (*c*) model 3, two-layer model with water-filled voids.

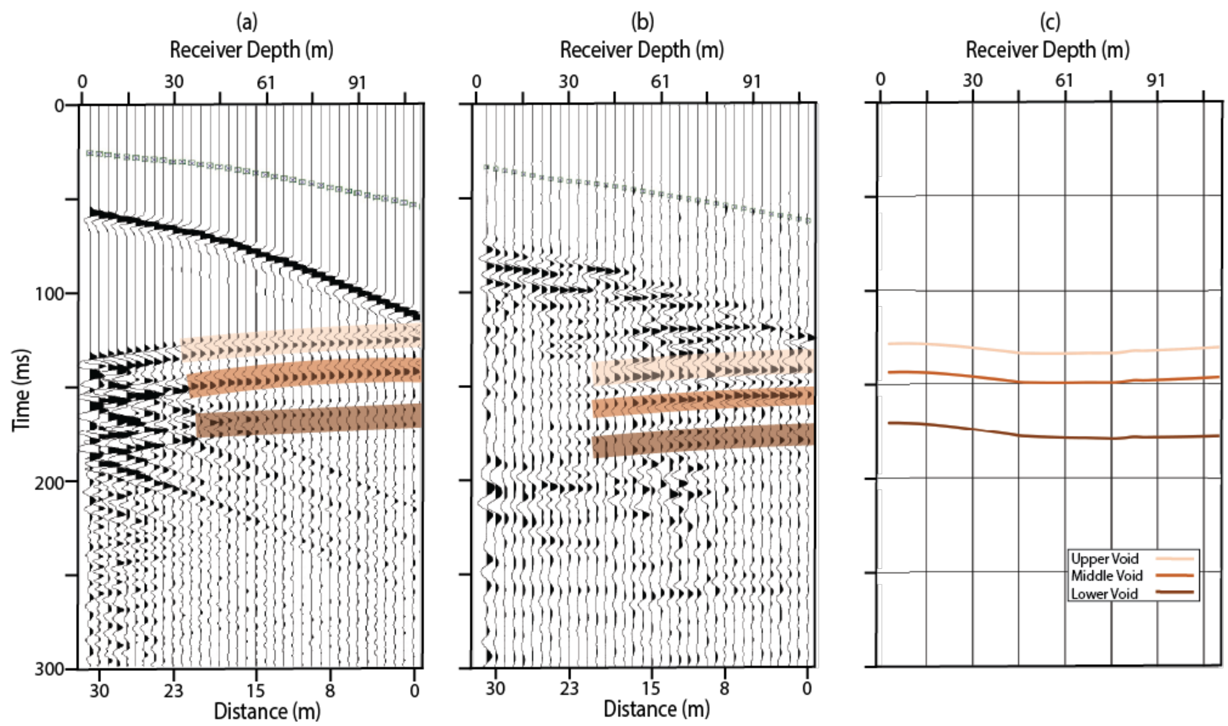

Figure 4. (*a*) Synthetic VSP simulating the three voids in well 2A (shown in Figure 3*c*). (*b*) VSP from February 2023 survey in well 2A. (*c*) Arrival times of diffractions from the three voids calculated using the velocity profile and depth of the void tops. Highlighting indicates interpreted diffractions from the three voids.

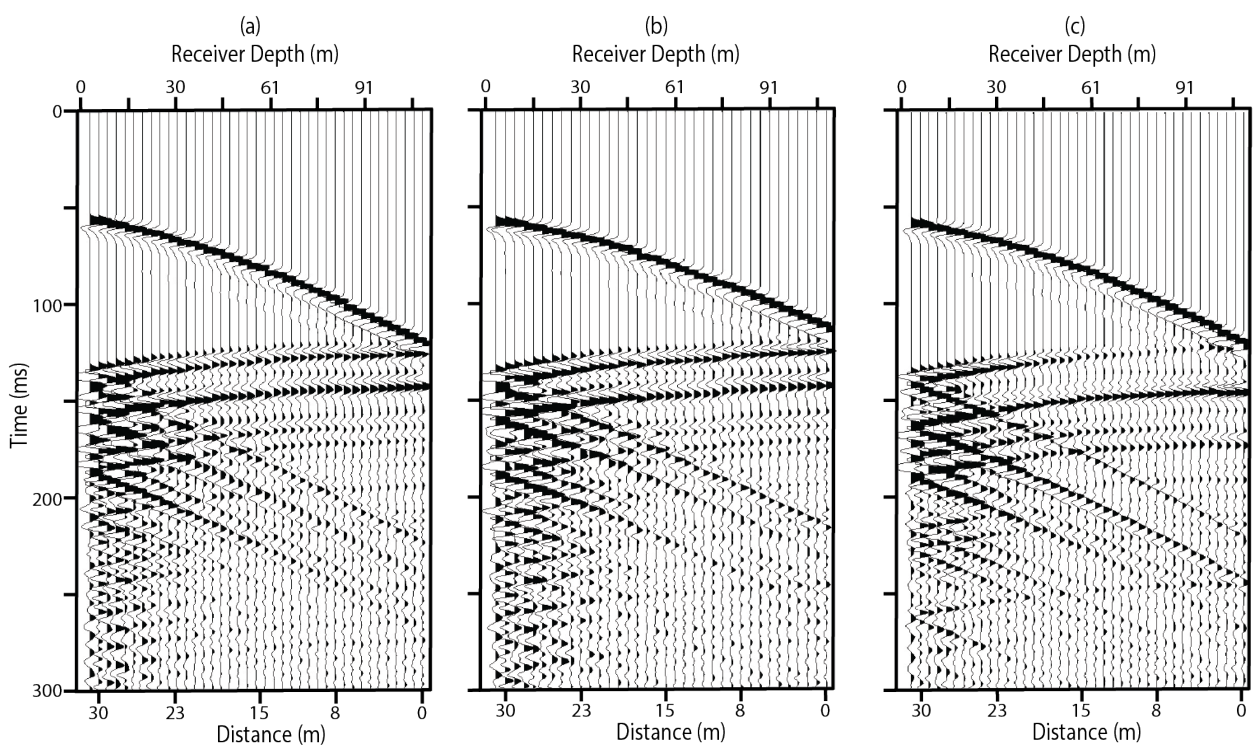

Figure 5. Synthetic VSPs from (*a*) model 3, representing baseline conditions; (*b*) model 4, horizontal growth of the upper void, and (*c*) model 5, vertical growth of the upper void.

Acquisition and Processing

A follow-up offset VSP survey was collected at well 2A on September 25, 2024 (Figure 6). The vertical source was a 16 lb. sledgehammer impacting a seated steel plate. The source location was 60 m due west and slightly south of well 2A, in approximately the same location as the baseline survey in February 2023. The downhole receiver was a three-component (3-C) Geostuff BHG-2 geophone with steel band clamping mechanism. Multipurpose rubber coating was applied to the exterior housing of the downhole tool and weatherstripping was applied to the band prior to the baseline survey to improve coupling and reduce mechanical oscillations in the transverse direction. Because those enhancements were intended to improve signal in the shear-wave VSPs, they had not been replaced prior to the 2024 compressional only survey, despite notable wear. The receiver was incrementally lowered and clamped to the casing wall at 3 m intervals down to a maximum depth of 109 m. A minimum of three consecutive shots were acquired and individually saved at each depth to ensure sufficient signal.

Downhole data were processed with conventional VSP techniques (Hardage, 1985b) using SeisUtilities software developed at the KGS. Consecutive shots at each station were vertically stacked during processing to maximize S/N. The P-wave first breaks were picked on vertical-component traces. Frequency-wavenumber (*f-k*) and bandpass filters were applied to attenuate down-going waves and enhance reflected signal, respectively. Finally, static corrections based on first arrival times were applied to flatten reflections with a narrow *f-k* filter applied to attenuate sloping noise in the upgoing direction (Figure 7).

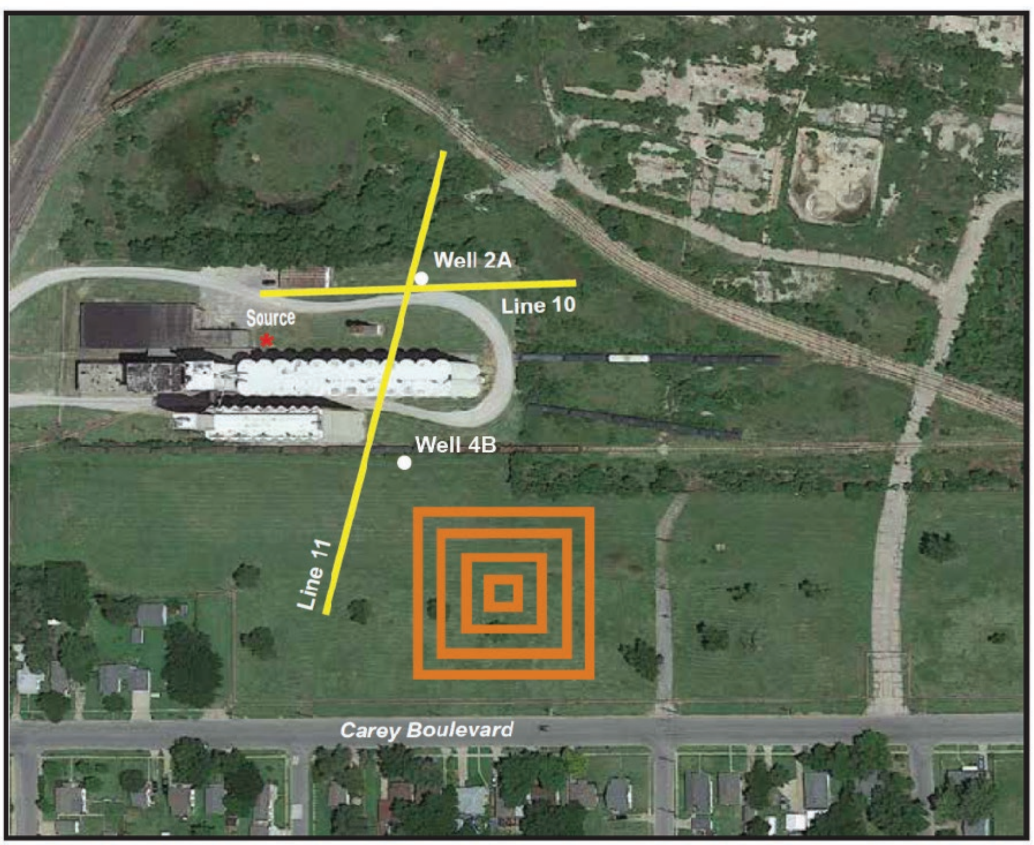

Figure 6. Layout of VSP surveys relative to wells 2A and 4B.

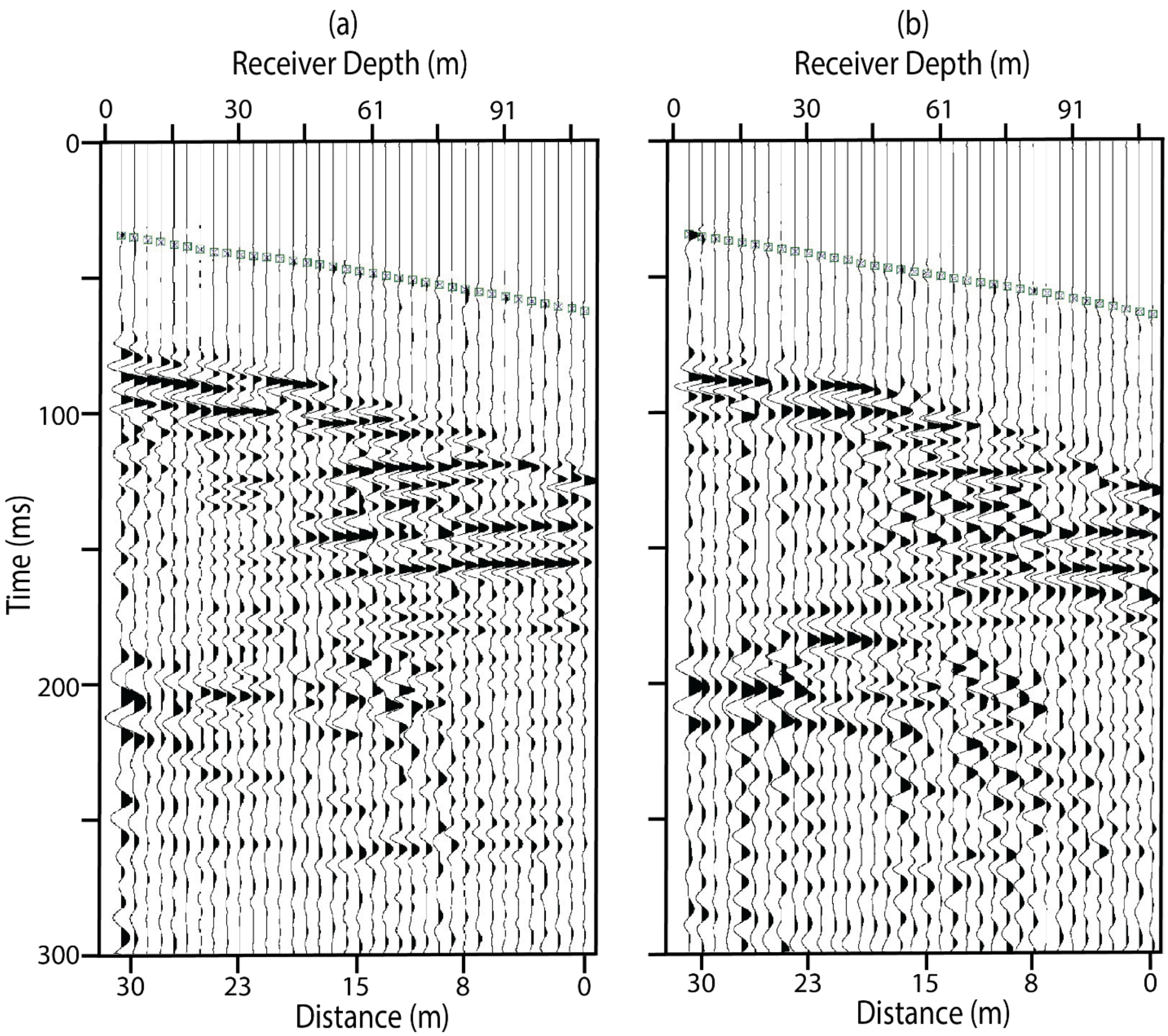

Figure 7. VSP in well 2A from (*a*) the baseline February 2023 survey, and (*b*) the time-lapse 2024 survey.

Results and Discussion

Seismic models are consistent with and strongly support our original interpretation that the event at 140 ms is likely a reflected/diffracted P-wave from the top of salt and top of the upper void (Figure 4). Any horizontal growth of the void would cause subtle changes in amplitude and phase characteristics of the diffraction and none were evident. Vertical migration would decrease the arrival time of the diffraction, causing destructive interference with the top of salt reflection and notable change in the resulting amplitude. These characteristics were not observed in time-lapse VSPs from well 2A. The arrival time of the diffraction from the upper void is about 140 ms in both the 2023 and 2024 surveys, and the size and shape of this event is approximately the same (Figure 7). Poor coherency of energy diffracted from the upper void at receiver depths of 50-85 m is probably related to variable cement bond quality within this interval. This degradation in coupling of the casing to the formation was indicated by acoustic amplitudes largely exceeding 20 mV in the cement bond log (where than 0.7 mV indicates 100% bonded and 81.2 mV indicates free pipe). Although coherency is subpar within this interval, seismic modeling indicates that diffraction amplitudes at receiver depths greater than 85 m would decrease as a result of vertical migration of the upper void. Lack of notable change in amplitude at these depths suggests little or no vertical growth at the time of the 2024 survey.

Vs calculated using passive surface wave analysis techniques at well 2A was elevated in the August 2024 survey, suggesting a period of increased stress. As noted above, the lack of amplitude changes in the upper void diffraction wavelet is evidence that no significant vertical migration has occurred between the acquisition of these two borehole data sets. Therefore, elevated Vs observed in the passive seismic is likely caused by changes in Young's Modulus due to increased stress but either (1) not yet at a level sufficient for macro strain (failure) instigating vertical migration of the roof, or (2) the strain resulted in failure and has been actualized through increases in the horizontal expanse of the cavern roof without measurable vertical change.

Conclusions

Relocation of the seismic source to the same location as the baseline survey improved source repeatability and overall quality of the time-lapse data. The arrival time of the top of salt reflection/upper void diffraction is about 140 ms in both the 2023 baseline and 2024 time-lapse surveys. The arrival time, amplitude, and phase characteristics of this event are consistent between surveys, suggesting little to no vertical growth has occurred since the baseline survey. Poor diffraction coherency between 50-85 m receiver depths is likely a result of variable cement bond quality within this interval. However, consistent amplitude and phase characteristics at receiver depths greater than 85 m support the interpretation that little to no vertical growth occurred between surveys. Seismic modeling suggests that while the VSP method is not particularly sensitive to horizontal growth of the void, it is quite sensitive to vertical migration, which represents the greatest hazard. This approach and tailored application of the method will allow direct detection of void migration, with continuous monitoring allowing accurate tracking and assessment of the potential for any future surface expression/breakthrough.

References

Dellwig, L.F., 1963, Environment and mechanics of deposition of the Permian Hutchinson Salt Member of the Wellington shale: Symposium on Salt, Northern Ohio Geological Society, p. 74-85.

Hardage, B.A., 1985a, Vertical Seismic Profiling: The Leading Edge, 4, 11, 59-60, https://doi.org/10.1190/1.1487141.

Hardage, B.A., 1985b, Vertical Seismic Profiling, Part A: Principles. *Geophysical Press*, 450 p.

Holdoway, K.A., 1978, Deposition of evaporites and red beds of the Nippewalla Group, Permian, western Kansas: Kansas Geological Survey Bulletin 215.

Kulstad, R.O., 1959, Thickness and salt percentage of the Hutchinson salt; *in* Symposium on Geophysics in Kansas: Kansas Geological Survey Bulletin 137, p. 241-247.

Levander, A. R., 1988, Fourth-order finite-difference P-SV seismograms: *Geophysics*, **53**, 1425–1436.

McGuire, D., and B. Miller, 1989, The utility of single-point seismic data; *in* Geophysics in Kansas, D.W. Steeples, ed.: Kansas Geological Survey Bulletin 226, p. 1-8.

Merriam, D.F., 1963, The Geologic History of Kansas: Kansas Geological Survey Bulletin 162, 317 p.

Merriam, D.F., and C.J. Mann, 1957, Sinkholes and related geologic features in Kansas: *Transactions of the Kansas Academy of Science*, v. 60, p. 207-243.

Miller, R.D., 2011, Progress report: 3-D passive surface-wave investigation of solution mining voids in Hutchinson, Kansas: Interim report to Burns & McDonnell Engineering Company, January, 9 p.

Peterie, S.L., J. Ivanov, M. Tamburro, R.D. Miller, B. Wedel, C. Bunker, C. Umbrell, 2023, Downhole Survey and Vertical Seismic Profiling at the CBRA: Kansas Geological Survey, Open-File Report 2023-64.

Peterie, S.L., J. Ivanov, M. Tamburro, R.D. Miller, B. Wedel, R. Keiffer, C. Umbrell, C. Bunker, 2024, VSP and Passive Seismic Characterization of Salt Jugs at Well 2A in Hutchinson, Kansas: November 2023 (Part 2): Kansas Geological Survey, Open-File Report 2024-34.

Stewart, R.R., and J.P. DiSiena, 1989, The values of VSP in interpretation: *The Leading Edge*, 8, 12, 16-23, https://doi.org/10.1190/1.1439597.

Swineford, A., 1955, Petrography of upper Permian rocks in south-central Kansas: State Geological Survey of Kansas Bulletin 111, 179 p.

Walters, R.F., 1978, Land subsidence in central Kansas related to salt dissolution: Kansas Geological Survey Bulletin 214, 82 p.

Whittemore, D.O., 1989, Geochemical characterization of saltwater contamination in the Macksville sink and adjacent aquifer: Kansas Geological Survey Open-file Report 89-35.

Whittemore, D.O., 1990, Geochemical identification of saltwater contamination at the Siefkes subsidence site: Report for the Kansas Corporation Commission.

Virieux, J., 1986, P-SV wave propagation in heterogeneous media: Velocity-stress finite-difference method: *Geophysics*, **51**, 889–901.

Zeng, C., J. Xia, R. D. Miller, and G. P. Tsoflias, 2011, Application of the multiaxial perfectly matched layer (M-PML) to near-surface seismic modeling with Rayleigh waves: *Geophysics*, **76**, no. 3, T43–T55.